Supplementary Information

A complementary experimental and computational study on methanol adsorption isotherms of H-ZSM-5

Santhosh K. Matam[1,2,*], Lotfi Boudjema[1,3,4], Matthew Quesne[1,2,5],

James D. Taylor[6], C. Richard A. Catlow[1,2,3]

[1]UK Catalysis Hub, Research Complex at Harwell, Science and Technology Facilities Council, Rutherford Appleton Laboratory, OX11 0FA, UK

[2]Cardiff Catalysis Institute, School of Chemistry, Cardiff University, Cardiff, CF10 3AT, UK

[3]Department of Chemistry, University College London, 20 Gordon St., London WC1E 6BT, UK

[4]ICGM, Univ. Montpellier, CNRS, ENSCM, Montpellier, France

[5]School of Chemistry, University of Leeds, Leeds LS2 9JT, UK

[6]ISIS Pulsed Neutron and Muon Facility, Science and Technology Facilities Council, Rutherford Appleton Laboratory, OX11 0QX, UK

*Corresponding author: santhosh.matam@rc-harwell.ac.uk;

Website: www.ukcatalysishub.co.uk

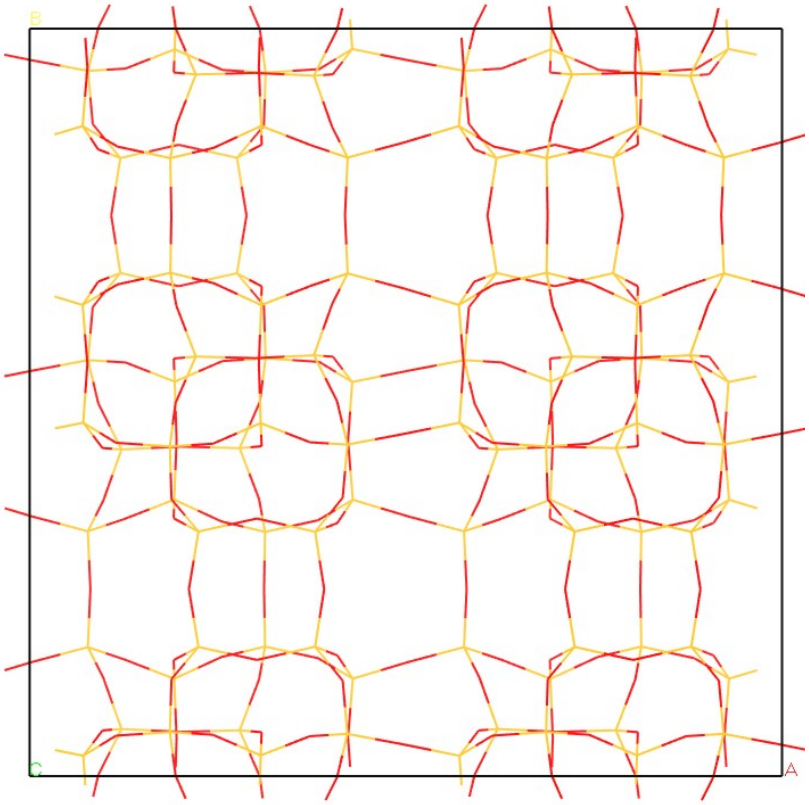

Fig. S1. MFI framework structure

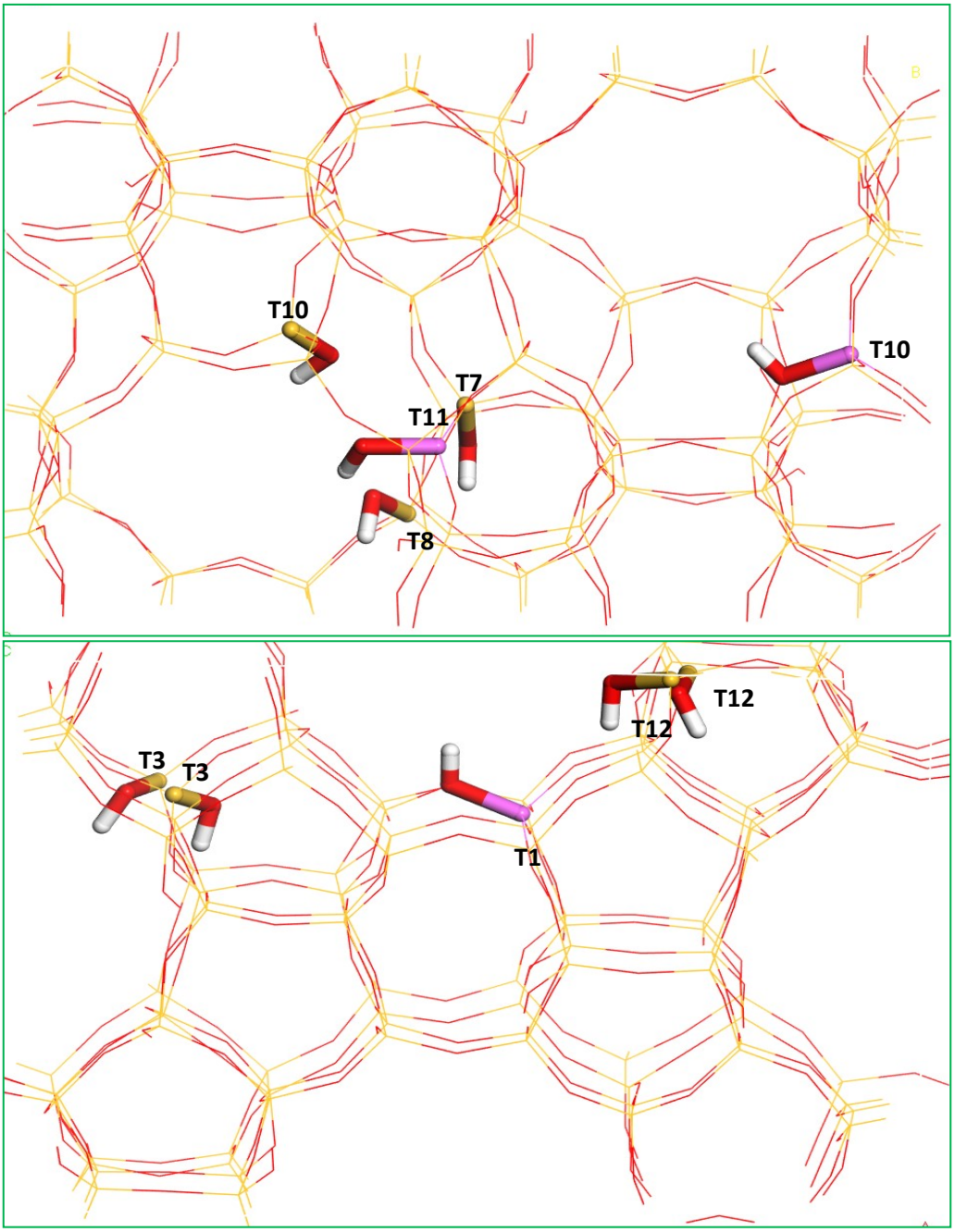

Fig. S2. Models of the fresh F-ZSM-5 (above) and steamed S-ZSM-5 (below) zeolites with different crystallographic sites than those reported in Fig. 4 (see the main article). The yellow, pink, red and grey denote Si, Al, O and H, respectively.

The models in Fig. S2 include T7, T8, T10 and T11 sites in F-ZSM-5 and T1, T3 and T12 in S-ZSM-5. Among these sites, T1, T8 and T12 sites match with our earlier work [1-3]. Additionally, we have also tested T2, T5 and T6 sites. None of these models describe the

experimental methanol adsorption isotherms (see Fig. S7), indicating the sensitivity of the sites.

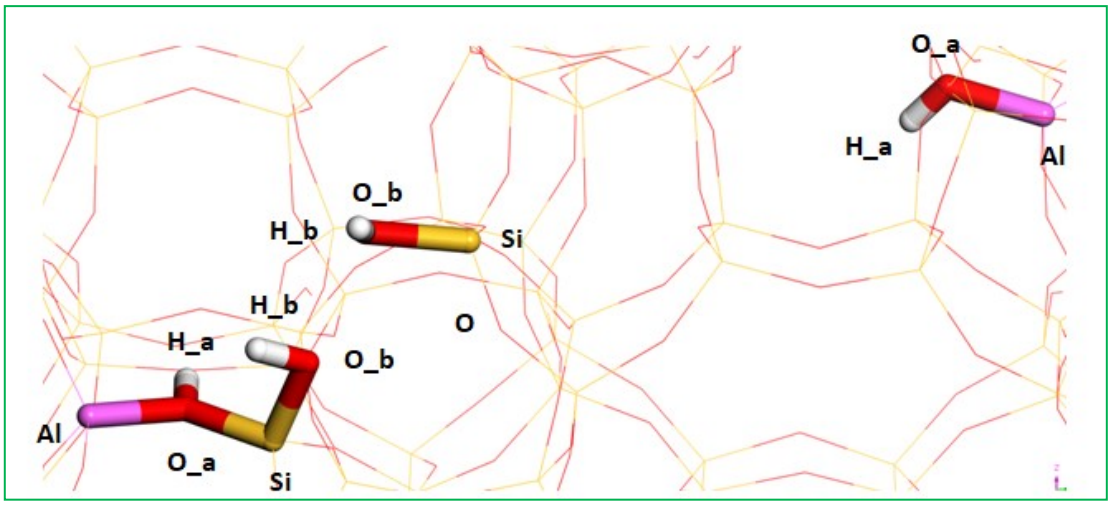

Fig. S3. The fresh F-ZSM-5 model.

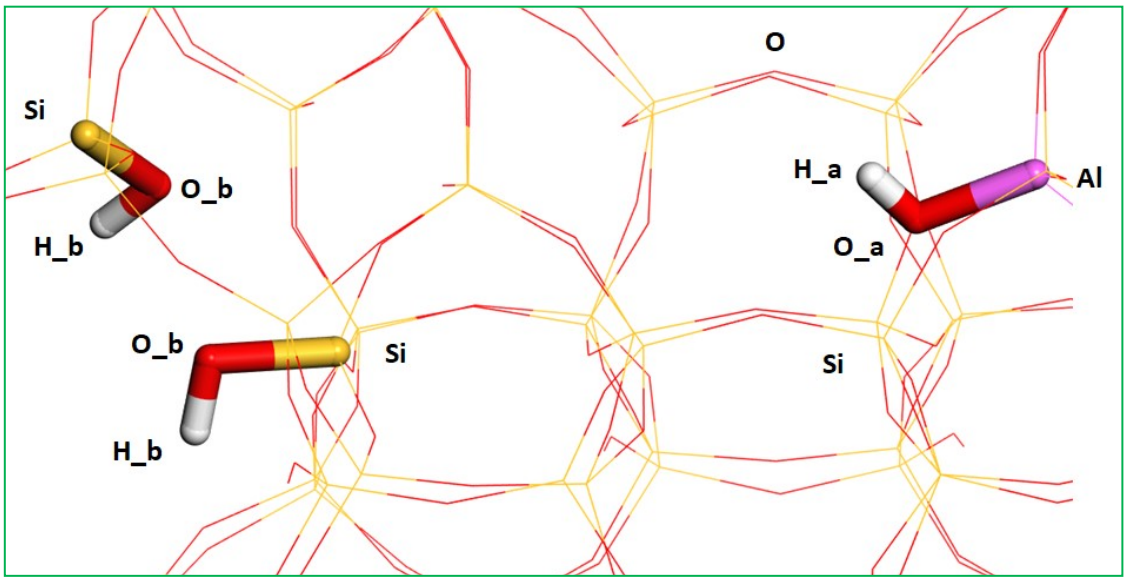

Fig. S4. The steamed S-ZSM-5 model.

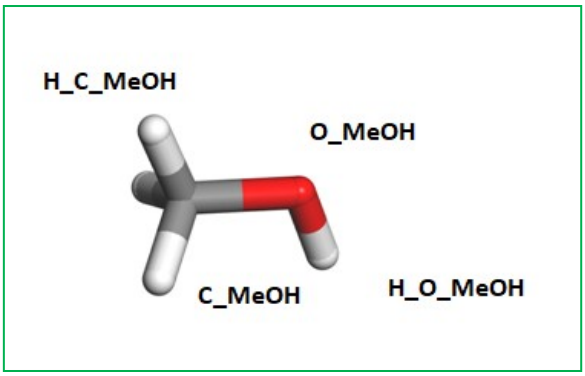

Fig. S5: The methanol molecule model.

Table S1. Potential parameters describing the zeolite-zeolite interactions

Buckingham potential			
Atoms	**A (eV)**	**ρ (Å)**	**C (eV Å^6)**
Si- -O	1283.907	0.32052	10.66158
Si- -O_a/O_b	983.5566	0.32052	10.66158
O- -O	22764.0	0.149	27.88
Al- -O	1460.3	0.29912	0
Al- -O_a	1142.6775	0.29912	0
Ob- -O	22764.0	0.29912	27.88
O- -H_a/H_b	311.97	0.25	0
Morse potential			
Atoms	**D (eV)**	**α (Å^{-1})**	**r_0 (Å)**
O_a- -H_a	7.0525	2.1986	0.9845
O_b- -H_b	7.0525	2.1986	0.9845
Three-body potential			
Atoms	**K (eV rad^{-2})**	**θ(°)**	
O-Al-O/O_a/O_b	2.09724	109.47	
O-Si-O/O_a/O_b	2.09724	109.47	

Table S2. Potential parameters describing intramolecular methanol interactions, where O-MeOH and H-MeOH are the methanol hydroxyl oxygen and hydrogen respectively.

Intramolecular potentials		
Bonds	**k (eV Å^{-2})**	**Length (Å)**
C_MeOH -- H_C_MeOH	29.56	1.105

C_MeOH -- O_MeOH	33.33	1.420	
H_C_MeOH -- O_MeOH	46.97	0.945	
Angles	**k eV (rad^{-2})**	**θ(˚)**	
C_MeOH-O_MeOH-H_MeOH	5.6	108.32	
H_C_MeOH- C_MeOH-O_MeOH	5.5	106.9	
H_C_MeOH- C_MeOH- H_C_MeOH	4.4	108.38	
Dihedrals	**k eV (rad^{-2})**	**A**	**B**
H_C_MeOH- C_MeOH- O_MeOH - H_MeOH	0.00762	1.0	3.0

Table S3. Lennard-Jones potential parameters describing methanol-zeolite interactions.

Methanol – Zeolite interactions		
Atoms	**ε (eV)**	**σ (Å)**
O/O_a/O_b -- H_MeOH	0.004987	2.557
O/ O_a/O_b -- O_MeOH	0.010545	2.764
O/ O_a/O_b -- C_MeOH	0.006594	2.958
O/ O_a/O_b -- H_C_MeOH	0.004987	2.557
H_a/H_b -- H_MeOH	0.000851	1.784
H_a/H_b -- O_MeOH	0.00338	2.920
H_a/H_b -- C_MeOH	0.00299	2.806
H_a/H_b -- H_MeOH	0.000851	1.784

Table S4. Lennard-Jones potential parameters describing methanol-methanol interactions.

Methanol – Methanol interactions		
Atoms	**ε (eV)**	**σ (Å)**
H_C_MeOH — H_C_MeOH / H_MeOH	0.00165	2.450
H_C_MeOH -- C_MeOH	0.00338	2.920
H_C_MeOH -- O_MeOH	0.00404	2.650
O_MeOH- -O_MeOH	0.00988	2.860
O_MeOH-- C_MeOH	0.00828	3.150
O_MeOH—H_MeOH	0.00404	2.650
C_MeOH – H_MeOH	0.00338	2.920

Table S5. Atomic charges for the methanol molecule from [4].

Atoms	Label	Charge (e-)
C	C_MeOH	-0.093
H	H_C_MeOH	0.1
H	H_O_MeOH	0.225
O	O_MeOH	-0.432

The Lorentz-Berthelot combining rules were used to obtain the cross collision diameter and cross-well depth of the interaction energy.

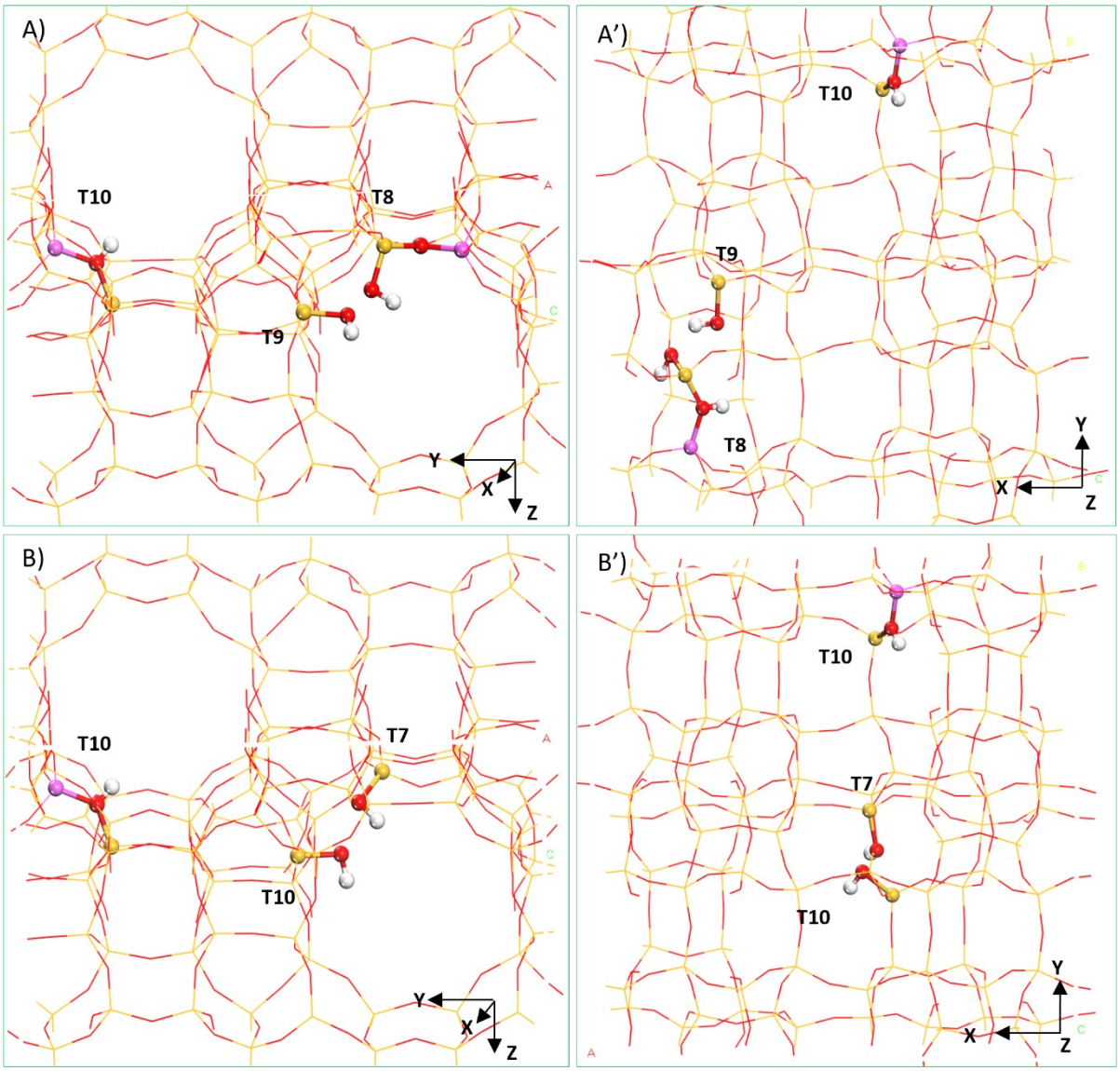

Fig. S6: Models depicting the location and orientation of the hydroxyl groups in the fresh F-ZSM-5 (A and A') and steamed S-ZSM-5 (B and B') zeolites from two different viewing directions. The yellow, pink, red and gray denote Si, Al, O and H, respectively.

F-ZSM-5 (A and A'): The T8 site comprises of both Brønsted and silanol hydroxyls which are neighbouring hydroxyls, and the site is located at an intersection of straight and sinusoidal channels and, the Brønsted hydroxyl is oriented in to a sinusoidal channel while the silanol hydroxyl is positioned in a straight channel. The silanol group at the T9 site is located at an intersection and is oriented in a straight channel. The T10 site is an isolated Brønsted hydroxyl which is located within a sinusoidal channel.

S-ZSM-5 (B) and (B'): The T10 site is an isolated Brønsted hydroxyl which is within a sinusoidal channel. The two silanol hydroxyls at T10 and T7 sites are located within a sinusoidal channel and straight channel, respectively.

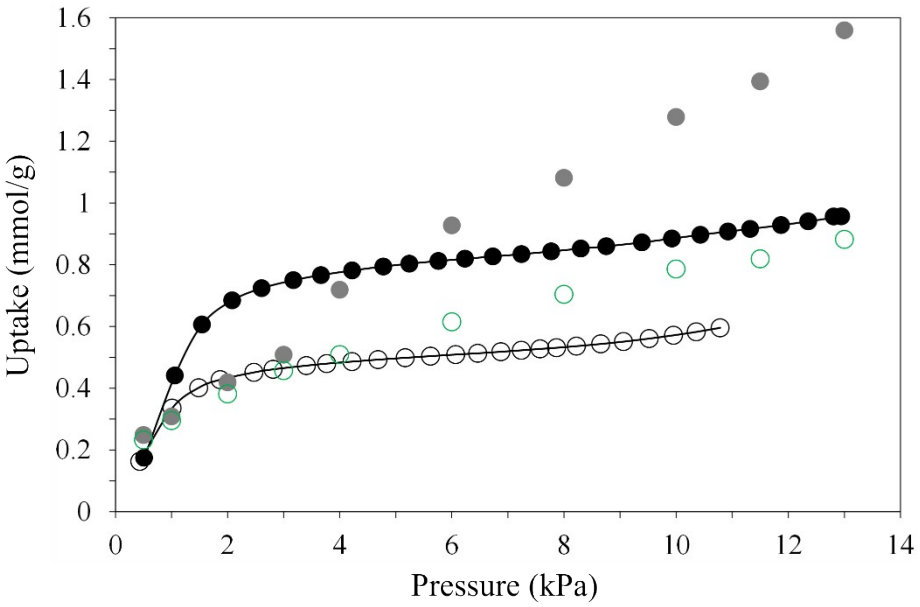

Fig. S7: Comparison of simulated methanol isotherms, using models depicted in Fig. S2, with experiments at room temperature. F-ZSM-5: filled symbols (Black: experimental and Gray: simulated) and S-ZSM-5 open symbols (Black: experimental and Green: simulated).

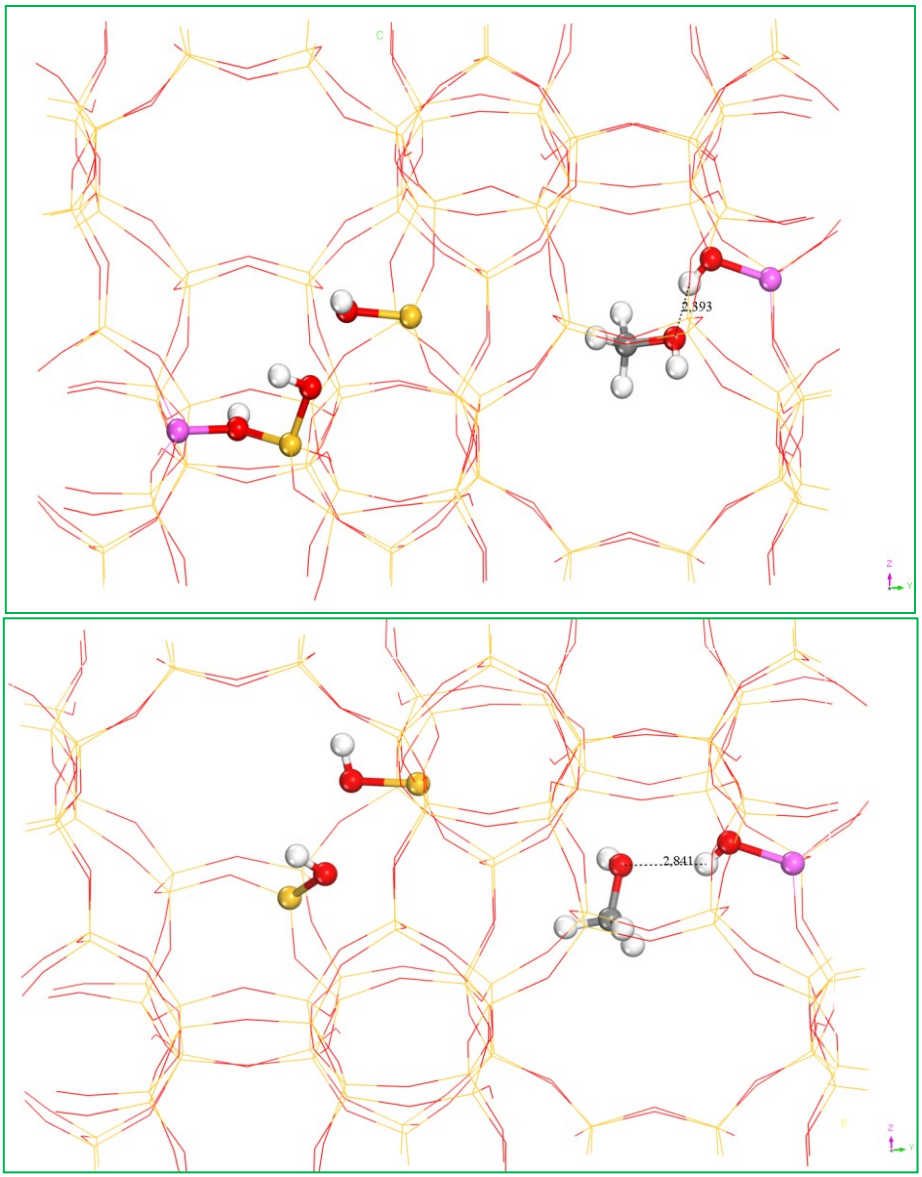

Fig. S8. Methanol adsorption enthalpies for one methanol molecule per unit cell are calculated by GCMC and the corresponding methanol configurations in F-ZSM-5 (above) and in S-ZSM-5 (below).

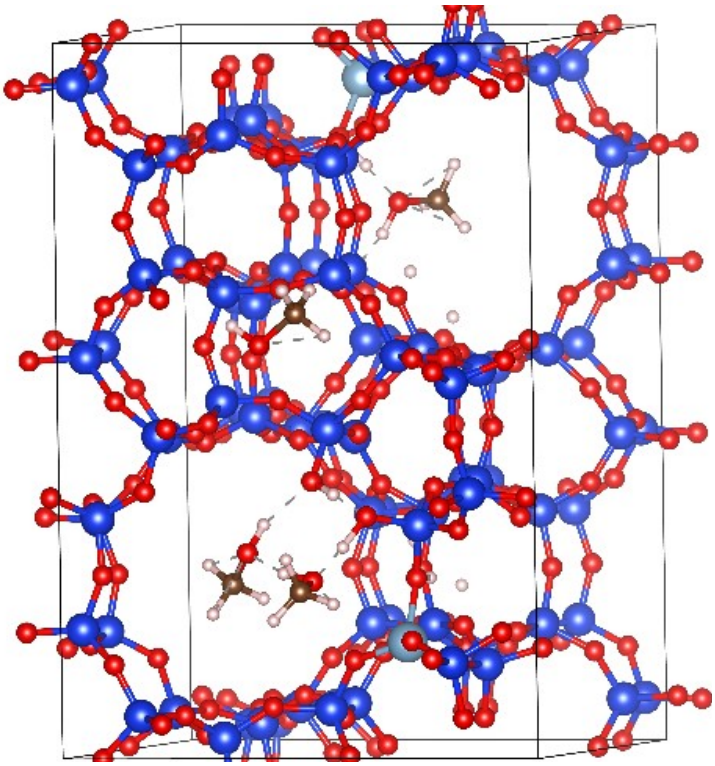

−335 kJ/mol

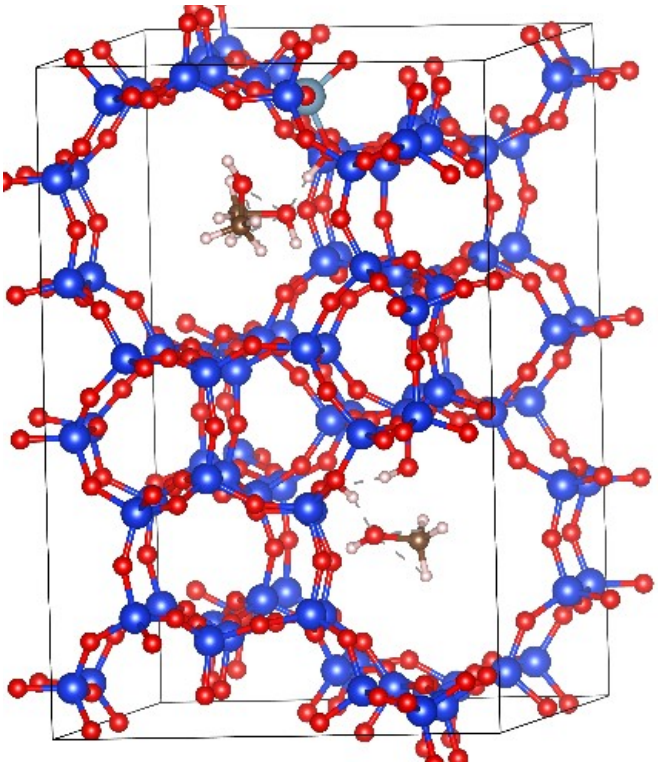

−229 kJ/mol

Fig. S9: Methanol adsorption geometry at 12.5 kPa. Methanol loading shown per unit cell for F-ZSM-5 (top) and S-ZSM-5 (bottom). Adsorption energies are given in kJ/mol relative to gas phase methanol and calculated at PBE level of theory. Colour scheme: blue, light blue, red and gray denote Si, Al, O and H

References:

[1] S. K. Matam, S. A. F. Nastase, A. J. Logsdail, C. Richard. A Catlow, Chem. Sci.11 (2020) 6805–6814. https://doi.org/10.1039/d0sc01924k
[2] S. A. F. Nastase, A. J. O'Malley, C. Richard. A Catlow, A. J. Logsdail, Phys. Chem. Chem. Phys. 21 (2019) 21, 2639-2650. https://doi.org/10.1039/c8cp06736h
[3] S. A. F. Nastase, P. Cnudde, L. Vanduyfhuys, K. De Wispelaere, V. Van Speybroeck, C. Richard A. Catlow, Andrew J. Logsdail, ACS Catal. 10 (2020) 8904–8915. https://doi.org/10.1021/acscatal.0c01454.
[4]. A. J. O'Malley, V. G. Sakai, I. P. Silverwood, N. Dimitratos, S. F. Parker, C. R. A. Catlow, Phys. Chem. Chem. Phys. 18 (2021) 17294–17302. https://doi.org/10.1039/C6CP01151A